Phase diagrams of mixtures of diastereomeric salts of N-acyl amino acid-type surfactants and separation of enantiomers

Phase Diagrams of Mixtures of Diastereomeric Salts of *N*-Acyl Amino Acid-Type Surfactants and Separation of Enantiomers

Akio Ohta,* Yoshitoki Hata, Yusuke Mizuno, Tsuyoshi Asakawa, and Shigeyoshi Miyagishi

Division of Material Sciences, Graduate School of Natural Science and Technology, Kanazawa University, Kanazawa, Ishikawa 920-8667, Japan

Received: April 27, 2004; In Final Form: June 8, 2004

An amino acid surfactant having an optically active base as a counterion was synthesized by neutralization of *N*-acyl amino acid with 1-phenylethylamine (PEA). Phase diagrams of diastereomeric mixtures of *R*-PEA *N*-acyl DL-amino acid and *RS*-PEA *N*-acyl D-amino acid systems were obtained by differential scanning calorimetry. The functions of *N*-acyl amino acids and PEA as optical resolving agents were examined by drawing the phase diagrams. FT-IR studies suggested that the difference in the magnitude of the interaction between the amide groups was a dominant factor affecting the difference in the physicochemical properties between the diastereomers.

Introduction

N-Acyl amino acid surfactants are of immense importance both from industrial and from domestic points of view, because of their biodegradability and low toxicity.[1] Furthermore, the chiral effect of *N*-acyl amino acid surfactants is interesting from the standpoint of physicochemical properties. There are two types of chiral discrimination: one in which the D−L interaction is more favorable, and a second where the D−D or L−L interaction is more favorable. It is known that the chiral discrimination of *N*-acyl amino acid surfactants in concentrated molecular organizations such as solids,[2−5] liquid crystals,[6,7] and condensed interfacial films[8−13] is remarkable. This effect in micelles, however, is much smaller than in the above cases.[14]

Generally, *N*-acyl amino acid was prepared as a surfactant after neutralization with a base. If an optically active base is used as the base in this situation, some physicochemical properties of the L-form of the *N*-acyl amino acid surfactant are different from those of the D-form, because these surfactant salts are diastereoisomers of each other. Although diastereomer-type surfactants originating from amino acids are of great interest as research targets, their micellar properties have never been studied. Another important feature of diastereomer-type surfactants is the function of the optical resolution of a racemate.[15] Resolution by diastereomeric salt formation is one of the most essential methods for producing a single enantiomer of a compound. The principle is very simple: the members of a pair of diastereomeric salts formed by reaction of a racemic acid or base with an optically active base or acid can be separated because of their different properties. If the equimolar mixture of the diastereomeric salts forms a solid solution or a compound, however, they cannot be purified in one step. In these instances, it is useful to construct phase diagrams of the binary isomeric mixture, to achieve enantiomeric resolution.[16] Furthermore, it is also important to examine the phase behavior in a solvent, because the separation is generally carried out by recrystallization from solution. Because the solubility of a surfactant increases abruptly at the Krafft temperature, which is the minimum temperature at which micellar particles can be formed in aqueous solution, it is reasonable to use a diastereomeric salt as a surfactant for enantiomeric resolution by recrystallization.

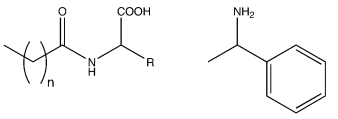

N-acyl amino acid
n = 12 (C14)
n = 14 (C16)

PEA

amino acid	residue (-R)
Ala	$-CH_3$
PheG	$-C_6H_5$
Phe	$-CH_2C_6H_5$

Figure 1. Chemical structures of the selected compounds.

Therefore, prior to studying the micellar properties of diastereomeric-type surfactants, this paper systematically investigates the phase behaviors of some binary mixtures of the diastereoisomers, by both differential scanning calorimetry (DSC) and conductometry. The latter method was employed to examine the phase behavior in the aqueous systems. We chose a diastereomer-type surfactant (see Figure 1) constructed by neutralization of *N*-acyl amino acid with 1-phenylethylamine (PEA). In addition, the difference in the interaction pattern between the diastereoisomers is discussed from the viewpoint of the hydrogen bonding of the amide group and the acid−base interaction, using vibration spectroscopy.

Experimental Section

Materials. L-Alanine and D-alanine (Ala), L- and D-phenylalanine (Phe), and L- and D-phenylglycine (PheG) were purchased from Peptide Institute, Inc. and Tokyo Chemical Industry Co., Ltd. *R*-1-Phenylethylamine and *S*-1-phenylethylamine (PEA) were purchased from Tokyo Chemical Industry Co., Ltd. To avoid confusion, we discriminate between the optically active isomers of the amino acid by using D- or L-, and those of phenylethylamine by using *R*- or *S*-, respectively. All chemicals were used without further purification. *N*-Hexadecanoyl alanine (C16-Ala; see Figure 1) and *N*-tetradecanoyl phenylalanine and

* Corresponding author. E-mail: adio-o@t.kanazawa-u.ac.jp.

10.1021/jp048159b CCC: $27.50
Published on Web 07/16/2004

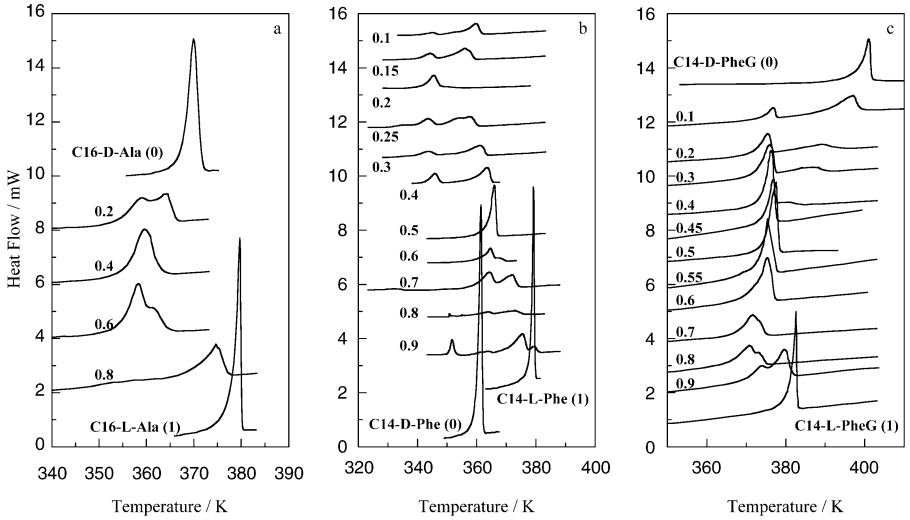

Figure 2. Thermograms for binary diastereomer mixtures. (a) *R*-PEA C16-D-Ala and *R*-PEA C16-D-Ala mixed system; (b) *R*-PEA C14-D-PheG and *R*-PEA C14-L-PheG mixed system; (c) *R*-PEA C14-D-Phe and *R*-PEA C14-L-Phe mixed system.

phenylglycine (C14-Phe, C14-PheG) were synthesized by the reaction of an amino acid with hexadecanoyl or tetradecanoyl chlorides as described previously[14] and were recrystallized from their mixtures in acetone−methanol. Their purities were checked by HPLC and DSC and by observing no minimum in the surface tension versus concentration curves at 298.15 K. 1-Phenylethylammonium *N*-acyl amino acid salts were obtained by neutralization of *N*-acyl amino acid with phenylethylamine in methanol.

Construction of Phase Diagrams. The phase diagrams of mixtures of diastereomeric salts were obtained by using differential scanning calorimetry (DSC). DSC experiments were carried out by using a DSC7 (Perkin-Elmer) thermal analyzer with a scanning rate of 4 K min^{-1}. Mixtures of different compositions were prepared by weighing different amounts of each component into glass test tubes. Mixing of the substances was achieved by dissolving them in methanol. After each sample was dried under reduced pressure to remove the solvent, some of it was sealed in an aluminum pan.

Electric Conductivity. Electric conductivities of the aqueous solutions of some diastereomeric salts (e.g., *R*-PEA C16-L-Ala, *R*-PEA C16-D-Ala), and their 1:1 mixtures (e.g., *R*-PEA C16-DL-Ala, *RS*-PEA C16-D-Ala) with coexisting solid samples, were measured as a function of temperature and preparation concentration by using a TOA electrode (CG-511B).

Specific Rotation. Specific rotations of some diastereomeric salts were measured on a HORIBA SEPA-300 spectrometer at 298.2 K. The wavelength and the path length were 589 nm and 1 cm, respectively. The sample was prepared as a 10 mM solution in ethanol.

FT-IR. Infrared absorption spectra were measured on a JASCO plus 460 spectrometer by the KBr disk method. Sixteen scans were accumulated at a resolution of 1 cm^{-1}.

Results and Discussion

The melting points and the enthalpies of fusion of the diastereomeric salts were obtained from the thermograms accompanying the fusion of the solid. These values are shown in Table 1. It can be seen that the melting points of the enantiomers are consistent with each other (e.g., *R*-PEA C16-L-Ala and *S*-PEA C16-D-Ala), while those of the diastereomers differ from each other (e.g., *R*-PEA C16-L-Ala and *R*-PEA C16-D-Ala). Similar results were obtained for the other amino acid derivatives.

TABLE 1: Melting Temperatures and Enthalpies of Fusion of Several Surfactants

	melting temperature/K		enthalpy of fusion/kJ mol^{-1}	
	R-PEA	*S*-PEA	*R*-PEA	*S*-PEA
C16-L-Ala	378.5	367.2	49.1 ± 2.2	63.6 ± 2.9
C16-D-Ala	367.8	378.2	62.6 ± 3.7	49.4 ± 1.4
C14-L-PheG	381.2	399.7	38.1 ± 2.6	32.6 ± 3.5
C14-D-PheG	399.0	381.0	33.9 ± 2.6	38.3 ± 0.9
C14-L-Phe	380.6	360.2	38.3 ± 1.7	50.3 ± 1.8
C14-D-Phe	360.3	380.9	51.3 ± 3.1	39.1 ± 2.0

Phase Diagrams of Mixed Diastereoisomer Systems. The melting curves obtained for the mixtures of *R*-PEA *N*-acyl L-amino acid and *R*-PEA *N*-acyl D-amino acid are presented in Figure 2. The solidus values were obtained from the peak onset temperatures, and the liquidus values were obtained from the offset temperatures modified by the shape factors.[16] The binary phase diagrams were constructed by plotting these two values against the mole fraction and are shown in Figure 3. If these components are ideally miscible in the liquid state, but completely immiscible in the solid state, the coexistence curve of the solution with crystals of component *i* is given by

$$\ln x_i^l = -\frac{\Delta_f h_i^0}{R}\left(\frac{1}{T} - \frac{1}{T_i^0}\right) \quad (1)$$

where x_i^l is the mole fraction of component *i* in the solution, and $\Delta_f h_i^0$ and T_i^0 are the molar enthalpy of fusion, which is assumed to be independent of temperature, and the melting point of pure component *i*, respectively. The dotted line in Figure 3a is calculated using eq 1, and it reproduced the experimental data sufficiently. Therefore, it is seen that no compound is formed at whole mole fraction in the *R*-PEA C16-DL-Ala mixed diastereoisomer system, and *R*-PEA C16-L-Ala is completely immiscible with *R*-PEA C16-D-Ala in the solid state. On the other hand, in both the *R*-PEA C14-DL-PheG and the *R*-PEA C14-DL-Phe mixed diastereoisomer systems, the compound formed by an equimolar mixture of counterparts appears and is immiscible with the pure components in the solid state. These results indicate that C16-L-Ala could be obtained by recrystallization of the racemic salt with *R*-PEA, while the racemates of C14-DL-PheG and C14-DL-Phe cannot be purified by diastereomeric salt formation with PEA, if their crystal structures in the solvent are kept even.

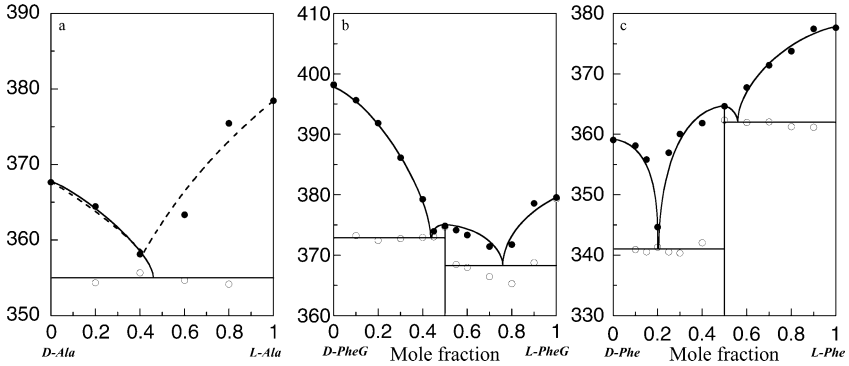

Figure 3. Phase diagrams for binary diastereomer mixtures. (a) *R*-PEA C16-D-Ala and *R*-PEA C16-L-Ala mixed system; the dotted lines were calculated using eq 1; (b) *R*-PEA C14-D-PheG and *R*-PEA C14-L-PheG mixed system; (c) *R*-PEA C14-D-Phe and *R*-PEA C14-L-Phe mixed system. (○) solidus, (●) liquidus.

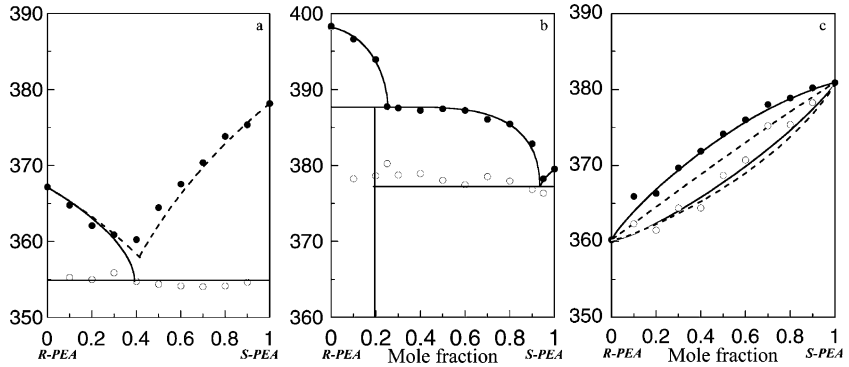

Figure 4. Phase diagrams for binary diastereomer mixtures. (a) *R*-PEA C16-D-Ala and *S*-PEA C16-D-Ala; (b) *R*-PEA C14-D-PheG and *S*-PEA C14-D-PheG; (c) *R*-PEA C14-D-Phe and **S**-PEA C14-D-Phe; the dotted lines were calculated using eq 2. (○) solidus, (●) liquidus.

Next, we examined phase behaviors of the mixtures of *R*-PEA *N*-acyl D-amino acid and *S*-PEA *N*-acyl D-amino acid. Figure 4 shows their phase diagrams constructed by using the liquidus and solidus values, respectively. It can be seen that the *RS*-PEA C16-D-Ala mixed diastereoisomer system does not form a compound at whole mole fraction, and neither does the *R*-PEA C16-DL-Ala mixed diastereoisomer system. In contrast, the phase behaviors of the *RS*-PEA C14-D-PheG and *RS*-PEA C14-D-Phe mixed diastereoisomer systems are completely different from those of the *R*-PEA C14-DL-PheG and *R*-PEA C14-DL-Phe mixed diastereoisomer systems. In the *RS*-PEA C14-D-PheG mixed diastereoisomer system, the composition of the compound is not equimolar, but about $X_S = 0.2$. On the other hand, no compound is formed in the *RS*-PEA C14-D-Phe mixed diastereoisomer system, and *R*-PEA C14-D-Phe is completely miscible with *S*-PEA C14-D-Phe in the solid state. The theoretical curves were obtained from the following van Laar equations for an ideal system and are shown in Figure 4c as dotted lines.

$$x_2^{\,l} = \frac{e^{\lambda_1} - 1}{e^{\lambda_1} - e^{\lambda_2}}; \quad x_2^{\,s} = \frac{e^{\lambda_1} - 1}{e^{\lambda_1 + \lambda_2} - 1} \tag{2}$$

where

$$\lambda_1 = \frac{\Delta_f h_1^{\,0}}{R}\left(\frac{1}{T} - \frac{1}{T_1^{\,0}}\right); \quad \lambda_2 = -\frac{\Delta_f h_2^{\,0}}{R}\left(\frac{1}{T} - \frac{1}{T_2^{\,0}}\right) \tag{3}$$

It is seen that the calculated and experimental curves are in relatively good agreement, showing that this system is nearly ideal. Consequently, the racemate of PEA can be purified by diastereomeric salt formation only when C16-Ala is used as the chiral acid.

TABLE 2: Krafft Temperatures by Conductivity Measurement at 10 mM

	Krafft temperature/K		
	R-PEA	*S*-PEA	*RS*-PEA
C16-L-Ala	313.8	310.3	
C16-D-Ala	310.6	314.6	303.8
C16-DL-Ala	299.3	299.1	
C14-L-PheG	321.8	329.7	
C14-D-PheG	329.6	322.8	318.8
C14-DL-PheG	326.2	327.4	
C14-L-Phe	306.4	309.5	
C14-D-Phe	308.5	306.9	295.6
C14-DL-Phe	294.1	294.9	

Electrical Conductivity. The electrical conductivities of 10 mM aqueous solutions of *R*-PEA *N*-acyl L-amino acid, *R*-PEA *N*-acyl D-amino acid, and *R*-PEA *N*-acyl DL-amino acid (equimolar mixture) in the presence of the solid deposit are shown in Figure 5. It can be seen that the electrical conductivity rises abruptly because of the complete dissolution of the surfactant around the Krafft temperature (KT). In this measurement, KT could be defined as the temperature corresponding to the inflection point, and these values are shown in Table 2. It is seen that the KT of one diastereomer is different from the other, while there is no difference in KT between enantiomers, similarly to the case for the melting temperature. The KT values of *R*-PEA C16-L-Ala and *R*-PEA C14-D-PheG were higher than the corresponding values of the other diastereoisomers. Because the trends in both KTs for the diastereomers are identical to those of the melting temperatures, their solid-state crystal structures seem to be maintained, even in aqueous solution. On the other hand, the KT of *R*-PEA C14-L-Phe, which had a higher melting point, was lower than that of *R*-PEA C14-D-Phe. For this system, therefore, it is possible that water molecules are

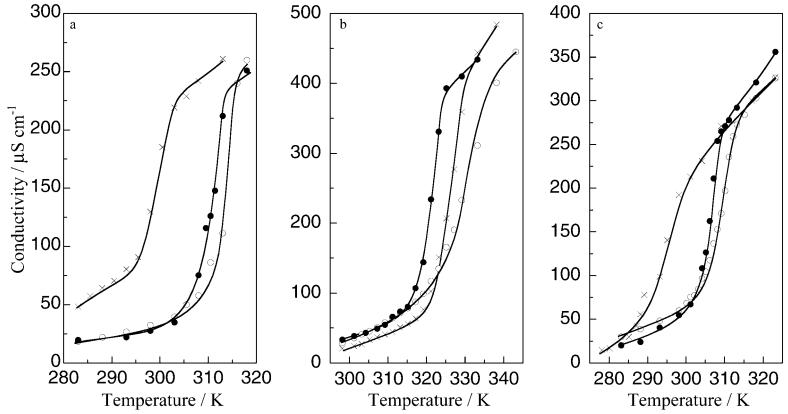

Figure 5. Electrical conductivity versus temperature curves. (a) *R*-PEA C16-Ala; (b) *R*-PEA C14-PheG; (c) *R*-PEA C14-Phe. (○) L-amino acid, (●) D-amino acid, (×) DL-equimolar mixture.

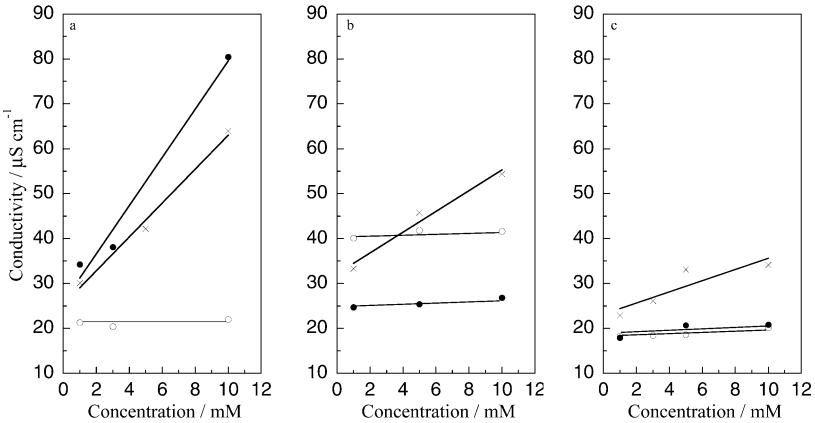

Figure 6. Electrical conductivity versus prepared concentration curves. (a) PEA C16-Ala at 293.2 K; (b) PEA C14-PheG at 303.2 K; (c) PEA C14-Phe at 283.2 K. (○) *R*-PEA L-amino acid, (●) DL-equimolar mixture, (×) *RS*-equimolar mixture.

TABLE 3: Specific Rotations of Several Isomers and Optical Purities of Racemates Before and After Resolution

	$[\alpha]_{589nm}^{298.2K}$				optical purity of L-form in racemate/%	
	D	L	DL	DL[a]	before resolution	after resolution
R-PEA C16-Ala	1.9	10.2	5.6	10.0	48	98
R-PEA C14-PheG	−64.6	77.7	6.4	3.2	51	48
R-PEA C14-Phe	−28.9	36.9	5.0	3.5	50	49
	$[\alpha]_{589nm}^{298.2K}$				optical purity of *S*-form in racemate/%	
	R	*S*	*RS*	*RS*[a]	before resolution	after resolution
PEA C14-D-PheG	−64.6	−71.2	−68.3	−65.8	52	18

[a] After recrystallization from its 10 mM aqueous solution.

incorporated into the surfactant crystal, changing the crystal structure. In fact, a monohydrate of *R*-PEA C14-L-Phe was obtained by recrystallization from its aqueous solution.[18]

We next examined the dependence of the electrical conductivity of the alanine-type surfactants on the prepared concentration at 293.2 K, which is below the KT, and these results are presented in Figure 6a. It is seen that the electrical conductivity, that is, solubility of *R*-PEA C16-L-Ala is independent of the concentration, while the corresponding properties of *R*-PEA C16-DL-Ala and *RS*-PEA C16-D-Ala, which are equimolar mixtures, are dependent on the concentration. This clearly shows that the degrees of freedom of the aqueous system of the equimolar mixtures of the diastereoisomers are at least larger than one, at constant temperature and pressure. Taking into account that the number of components of these systems is three, the number of phases in these systems must be less than two. This means that the solid coexisting with the aqueous solution of the equimolar mixture may be a pure component. The dependencies of the solubilities of the other systems of equimolar mixtures of diastereoisomers on the prepared concentration at a temperature below the KT are summarized in Figure 6b and c. For both *R*-PEA C14-DL-PheG and *R*-PEA C14-DL-Phe systems, the solubilities are independent of the concentration, and this can be explained by considering that the solids coexist as equimolar compounds. On the other hand, because the solid of *RS*-PEA C14-D-PheG is a compound with $X_R \neq 0.5$ and the corresponding solid of *RS*-PEA C14-D-Phe is a mixed crystal as mentioned above, these solubilities depend on the concentration.

Separation of Enantiomers. Separation of enantiomers from the racemates of *N*-acyl amino acid and PEA were examined by recrystallization of the 10 mM aqueous solutions of their diastereomeric salts. Their optical purities were checked by measuring specific rotation. Obtained data and calculated optical purities are shown in Table 3. It can be seen that the diastereomeric salts with higher melting temperatures deposit

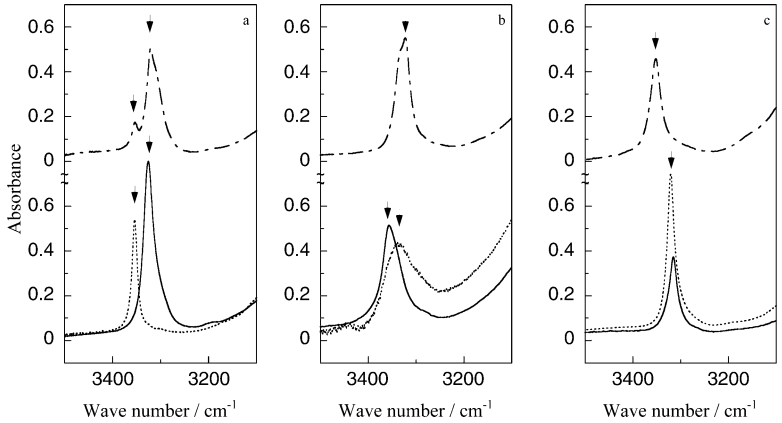

Figure 7. FT-IR spectra at the range of 3100−3500 cm^{-1}. (a) *R*-PEA C16-Ala; (b) *R*-PEA C14-PheG; (c) *R*-PEA C14-Phe. (solid line) L-amino acid, (dotted line) D-amino acid, (broken line) DL-equimolar mixture.

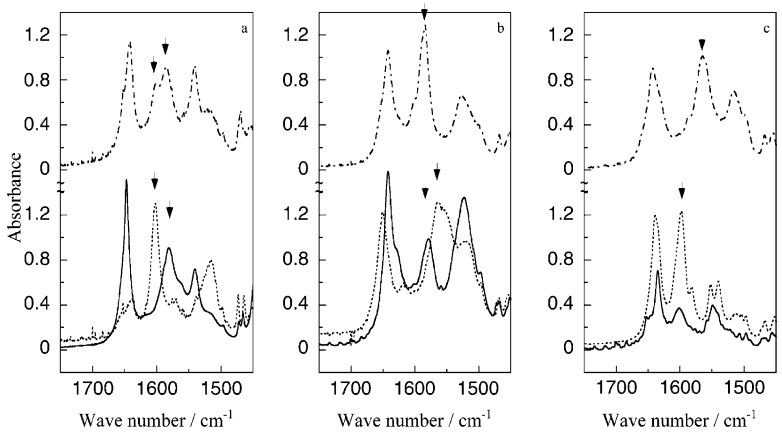

Figure 8. FT-IR spectra at the range of 1450−1750 cm^{-1}. (a) *R*-PEA C16-Ala; (b) *R*-PEA C14-PheG; (c) *R*-PEA C14-Phe. (solid line) L-amino acid, (dotted line) D-amino acid, (broken line) DL-equimolar mixture.

prior to the others in an equimolar solution of the *R*-PEA C16-DL-Ala system. For the racemates of C14-Phe and C14-PheG, the optical purities do not change by simple recrystallization of their diastereomeric PEA salts, because the equimolar mixtures exist as equimolar compounds even in aqueous solution. On the other hand, in the case of the *RS*-PEA C14-D-PheG mixed diastereoisomer system, the compound at $X_S = 0.2$ was obtained by recrystallization. These results were completely consistent with those expected by inspection of the phase diagrams.

Intermolecular Interaction in the Solid State. Kitoh et al. succeeded in obtaining the crystal structure of *R*-PEA C14-L-Phe by X-ray structural analysis.[18] In that study, it was reported that hydrogen bonding between the amide groups formed chained networks and that the carboxyl groups interacted helically with the amino groups. Therefore, it is worth examining the hydrogen bonding between the amide groups and the interaction between the acid and base groups, to compare the intermolecular interaction between the diastereomers in the solid state. Figure 7 shows FT-IR spectra of *R*-PEA *N*-acyl D-, L-, and DL (equimolar mixture)-amino acids in the solid state in the 3500−3100 cm^{-1} region, where the key band, the N−H stretching vibration of the amide group, is shifted to a lower wavenumber by hydrogen bonding. It is seen from Figure 7a that the wavenumber of the absorption for *R*-PEA C16-L-Ala is lower than that for *R*-PEA C16-D-Ala. This suggests that the hydrogen-bonding ability between the amide groups of *R*-PEA C16-L-Ala, which has a higher melting temperature, is superior to that of *R*-PEA C16-D-Ala. Furthermore, the fact that the absorption for *R*-PEA C16-DL-Ala is a superposition of those for *R*-PEA C16-D-Ala and *R*-PEA C16-L-Ala strongly supports that *R*-PEA C16-L-Ala is completely immiscible with *R*-PEA C16-D-Ala in the solid state. For the case of *R*-PEA C14-Phe shown in Figure 7b, there were no significant differences between the D- and L-forms; only the absorption of the DL-form, which is the racemic compound, is shifted to a higher wavenumber. Similarly to the case of the *R*-PEA C16-Ala system, the wavenumber of the absorption of the salt with the higher melting temperature was lower than that of the other for *R*-PEA C14-PheG. The hydrogen-bonding ability of the DL-form was most favorable for the *R*-PEA C14-PheG system, contrary to that in the *R*-PEA C14-Phe system.

Figure 8 shows the same FT-IR spectra in the 1750−1450 cm^{-1} region, where the key band is the C═O stretching vibration of amide or carboxyl groups. The absorption bands around 1650 and 1580 cm^{-1} were assigned the C═O stretching of the carboxyl group and the C═O stretching vibration of the amide group (amide I), respectively. Although the difference in the absorption band of amide I between the diastereoisomers is tiny for all of the cases, it corresponds to that of the N−H stretching vibration. For both *R*-PEA C16-Ala and *R*-PEA C14-PheG, the band for the C═O stretching vibration of the carboxyl group of the more stable diastereoisomer was shifted to a lower wavenumber, due to a stronger interaction with the amino group of PEA, and this tendency is similar to that of the N−H stretching vibration. This suggests that the stabilities of these diastereoisomers are dominated by both hydrogen bonding of the amide group and acid−base interaction, for the *R*-PEA C16-Ala and *R*-PEA C14-PheG systems. In the case of *R*-PEA C14-Phe, on the other hand, there are no remarkable band distinctions between the diastereoisomers. It is presumed that

other factors, for example, the interaction between phenyl groups, not hydrogen bonding and acid−base interaction, contribute to the stability of the diastereoisomer. In the same way, it can be said that the driving forces for compound formation for *R*-PEA C14-DL-Phe and *R*-PEA C14-DL-PheG are the hydrogen bonding of the amide group and the acid−base interaction, respectively.

Conclusions

Phase diagrams of binary mixtures of diastereomeric salts of *N*-acyl amino acid-type surfactants were obtained by DSC measurements. Experimental results showed that for only the case of the mixed diastereoisomer system including C16-Ala, no compound is formed at whole mole fraction, and one diastereomeric salt is completely immiscible with the other in the solid state. On the other hand, in both the *R*-PEA C14-DL-PheG and *R*-PEA C14-DL-Phe mixed diastereoisomer systems, the compound formed by an equimolar mixture of counterparts appears. Therefore, the more stable diastereomeric salt was obtained from an equimolar aqueous solution for only the *R*-PEA C16-DL-Ala system. For the racemates of C14-Phe and C14-PheG, however, the optical purities do not change by simple recrystallization of their diastereomeric PEA salts, because the equimolar mixtures exist as equimolar compounds even in aqueous solution. It was suggested that hydrogen bonding between the amide groups was one of the dominant factors for the stability of diastereomers for PEA C16-Ala and PEA C14-PheG.

References and Notes

(1) Takehara, M. *Colloids Surf.* **1984**, *38*, 149−167.
(2) Miyagishi, S.; Matsumura, S.; Murata, K.; Asakawa, T.; Nishida, M. *Bull. Chem. Soc. Jpn.* **1985**, *58*, 1019−1022.
(3) Miyagishi, S.; Matsumura, S.; Asakawa, T.; Nishida, M. *Bull. Chem. Soc. Jpn.* **1986**, *59*, 557−561.
(4) Ohta, A.; Ozawa, N.; Nakashima, S.; Asakawa, T.; Miyagishi, S. *Colloid Polym. Sci.* **2003**, *281*, 363−369.
(5) Ohta, A.; Nakashima, S.; Matsuyanagi, H.; Asakawa, T.; Miyagishi, S. *Colloid Polym. Sci.* **2003**, *282*, 162−169.
(6) Sakamoto, K.; Hatano, M. *Bull. Chem. Soc. Jpn.* **1980**, *53*, 339−343.
(7) Sakamoto, K. *Mol. Cryst. Liq. Cryst.* **1980**, *59*, 59−71.
(8) Harvry, N. G.; Mirajovsky, D.; Rose, P. L.; Verbiar, R.; Arnett, R. M. *J. Am. Chem. Soc.* **1989**, *111*, 1115−1122.
(9) Stine, K. J.; Uang, J. Y.-J.; Dingman, S. D. *Langmuir* **1993**, *9*, 2112−2118.
(10) Gericke, A.; Hühnerfuss, H. *Langmuir* **1994**, *10*, 3782−3786.
(11) Parazak, D. P.; Uang, J. Y.-J.; Turner, B.; Stine, K. J. *Langmuir* **1994**, *10*, 3787−3793.
(12) Hoffmann, F.; Hühnerfuss, H.; Stine, K. J. *Langmuir* **1998**, *14*, 4525−4534.
(13) Zhang, Y. J.; Song, Y.; Zhao, Y.; Li, T. J.; Jiang, L.; Zhu, D. *Langmuir* **2001**, *17*, 1317−1320.
(14) Miyagishi, S.; Nishida, M. *J. Colloid Interface Sci.* **1978**, *65*, 380−384.
(15) Kozma, D. *CRC Handbook of Optical Resolutions via Diastereomeric Salt Formation*; CRC Press: Boca Raton, FL, 2002.
(16) Leitão, M. L. P.; Eusébio, M. E.; Maria, T. M. R.; Redinha, J. S. *J. Chem. Thermodyn.* **2002**, *34*, 557−568.
(17) Courchinoux, R.; Chahn, N. B.; Haget, Y.; Tauler, E.; Cuevas-Diarte, M. A. *Thermochim. Acta* **1988**, *128*, 45−53.
(18) Kitoh, S.; Kunimoto, K.; Ohta, A.; Hata, Y.; Asakawa, T.; Miyagishi, S. *Acta Crystallogr.* submitted.